High Energy Physics and Nuclear Physics

Volume 21, Number 1

Concept Design of a New Structure of 1.3GHz Single-Cell Superconducting Cavities

Zu Donglin

(Institute of Heavy Ion Physics, Peking University, Beijing, China)

This paper reports on a new design of single-cell superconducting cavities. It consists of two half-end cells of the 9-cell Beijing TESLA shape accelerating cavity. The ratio of the maximal surface electric field to accelerating gradient, E_p/E_{acc}, of the π mode of the 9-cell cavity was reduced to 2.024. The cell-to-cell coupling k is as high as 1.95%. The E_p/E_{acc} in the single-cell cavities was reduced to 1.8. The monopole, dipole, and quadrupole high-order modes (HOMs) were calculated using URMEL-T with the resistance-band model. In addition, the concept of the structure parameters of the niobium cavity introduced the condition of calculation reliability with the codes; the calculation reliabilities of URMEL and URMEL-T were also discussed.

Key words: superconducting RF, superconducting cavity, niobium cavity, accelerating mode, HOM.

1. INTRODUCTION

Superconducting RF (SRF) cavities have been investigated for nearly thirty years in the USA, Europe, and Japan. In the 1960s and 1970s, scientists tried muffinlike cavities but the accelerating gradient, E_{acc}, was limited to 1 MV/m or so due to multipacting barriers in the cavities. In the 1970s and 1980s, circular [1] and elliptical [2] cavities which eliminated multipacting [3,4] effects were invented, and a breakthrough in E_{acc} of SRF cavities was made. The first generation of practical SRF

Received November 2, 1995. Supported by the National Natural Science Foundation of China.

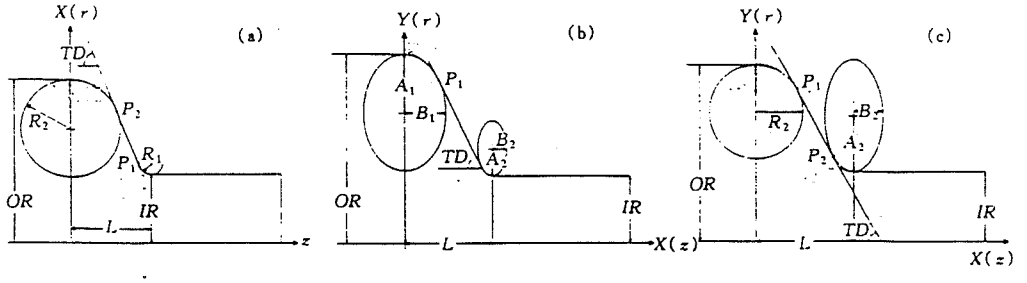

Fig. 1

Definition of superconducting cavity dimensions.
(a) circular cavity, (b) elliptical cavity, and (c) circular-elliptical cavity.

accelerating cavities, such as Cornell/CEBAF cavities, LEP cavities, HERA cavities, and Tristan cavities, etc., were developed. Their operating gradient, E_{acc}, is all 5 MV/m, but the empty load gradient distributes in the range of 7.5-15 MV/m. In the 1980s and 1990s, the concept of the TeV superconducting linear accelerator (TESLA) collider [5,6] based on the SRF cavity technique has been advanced, demanding the gradient of 20-40 MV/m. At present, field emission (FE) is the prevailing limitation to higher gradients. In order to overcome the obstacle, on the one hand, improving niobium purity to raise the residual resistivity ratio (RRR) could improve the thermal conductance and eliminate thermal breakdown. But considering yield intensity, RRR cannot be too high (about 300). On the other hand, processing the internal surface of the cavity wall can raise the field emission threshold, E_p. Using chemical polishing processing (CP), E_p could reach 30 MV/m [7] or higher. Using annealing processing with a titanium protective in a high vacuum furnace, E_p could reach 60 MV/m [8]. Using high RF peak power processing, E_p could reach 100 MV/m (the world record) [9]. Besides the two methods mentioned above, a third efficient way to raise E_{acc} is an optimum design of the SRF cavity geometric shape in which E_p/E_{acc} is as low as possible and then E_{acc} is as high as possible. As the target of TESLA, the cavity design is such that E_p/E_{acc} is reduced to 2.0, the cell-to-cell coupling k is larger than 1.8% (the higher the better), while the other characteristic parameters are not degraded.

URMEL [10] and URMEL-T [11] are powerful tools in the design of the SRF cavities. We have obtained three different cavity shapes via a thousand times of running the codes: BSC1, BSC2, and BSC3. BSC1 was developed based on analysis and comparison of individual cavities operating on-line such as Cornell/CEBAF and LEP cavities and newly designed cavities in other laboratories such as Cornell B-Factory and Milan's ARES. BSC2 and BSC3 are the combiners of the half-end cells of our newly designed 9-cell TESLA cavity (BT for short) [12]. The two shapes take their source at the different tuning methods.

2. DEFINITION OF SRF CAVITY GEOMETRY PARAMETERS

The structure parameters of a cavity are usually described using one-fourth of the lengthwise section of the SRF cavity with axial symmetry, where the cell is the elemental block of the cavity. The half-cell wall consists of several segments of curves, such as the circle–straight line–circle or the ellipse–straight line–ellipse. Hence, the cell shape can be divided into types of "CSC" and "ESE." The CSC type is shown in Fig. 1(a), where the main parameters are cell radius *OR*, equator circle radius R_2, beam tube radius *IR*, iris circle radius R_1, wall slope *TD*, and half-cell length L; six in total. The running of URMEL, URMEL-T, and SUPERFISH [13] codes requires an input file comprised of the six parameters. Machining a cavity needs to know the coordinate positions of two circle centers and

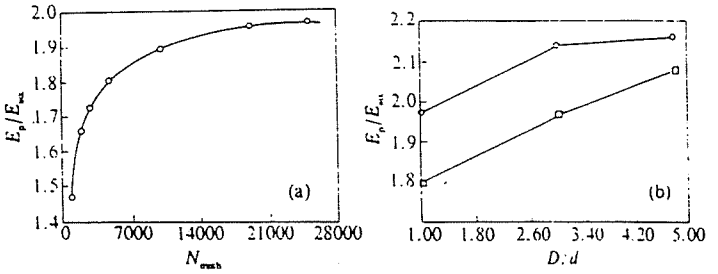

Fig. 2

E_p/E_{acc} calculated using URMEL versus mesh.
(a) E_p/E_{acc} is a function of number of mesh points and
(b) E_p/E_{acc} is a function of mesh density ratio D/d.
○ for ARES cavity; □ for BSC1 cavity.

two tangent points. The running of SHAPE codes only requires five parameters, e.g., *OR*, *IR*, R_1, *TD*, and *L*. The position of the equator circle center, the tangent points P_1, P_2, and the input file can be obtained through running the SHAPE codes.

The ESE type is shown in Fig. 1(b), where the main parameters are *OR*, *IR*, *TD*, A_1, B_1, A_2, and B_2; seven in total, respectively. A_1 and B_1 are the half axial lengths of the equator ellipse at $Y(r)$ and $X(z)$ directions, respectively, A_2 and B_2 are the half axial lengths of the iris ellipse at $Y(r)$ and $X(z)$ directions, respectively. The Cornell/CEBAF cavities belong to the ESE type, while LEP cavities are of the CSC type. The CSE type reported here was developed by the authors, its circle is at the equator area and its ellipse is at the iris, as shown in Fig. 1(c). Its main parameters are *OR*, R_2, *L*, *TD*, A_2, and B_2; six in total. This type has additional advantages over the above two types and overcomes their fatal disadvantages. In Fig. 1, there are two sets of coordinates, among them the *r*-*z* frame is used for URMEL and URMEL-T codes, and the *Y*-*X* frame is used for the SHAPE codes.

3. ISSUE OF CALCULATION RELIABILITY OF URMEL AND URMEL-T CODES

The calculation reliability of running URMEL and URMEL-T codes is worthy of discussion. The criterion is to check the consistency of output results from URMEL or URMEL-T. For example, $(R/Q)''$ fluctuates versus position R_0 [14] when it is calculated using 2,000 mesh points. However, $(R/Q)''$ no longer fluctuates versus R_0 when using 25,000 mesh points. This suggests that the former is not credible, but the latter is credible.

The accurate calculation of E_p/E_{acc} is more difficult. Experiences have shown that the calculated value of E_p/E_{acc} not only relates to the number of mesh points, but also to the mesh density ratio, and even relates to the codes. The lower the number of mesh points used, the farther the E_p/E_{acc} deviates from its true value. Conversely, the greater the number of mesh points used, the more accurate the E_p/E_{acc} is. Besides, the E_p/E_{acc} calculated using URMEL-T is always not credible because the maximal mesh points permitted by URMEL-T are only 7,000, while URMEL permits the maximum of 25,000 mesh points. For calculation of the ARES cavity, different results of E_p/E_{acc} corresponding to different mesh points are shown in Fig. 2(a). In addition, URMEL permits the technique of variable mesh density, e.g., dilute mesh is taken at beam tube, dense mesh is taken at the cell, the densest mesh taken at the iris where the maximal surface electric field E_p appears and varies fiercely, while keeping the total mesh points not beyond 25,000, so the probability to capture the maximal E_p could be raised. The maximal mesh density ratio permitted by URMEL is $D/d = 5{:}1$. Mesh density ratio $D/d = 1$ means automatic mesh. We have calculated E_p/E_{acc} of ARES cavity and BSC1 cavity using $D/d = 1, 3$, and 5, respectively; the results are shown in Fig. 2(b). It is easy to realize why the results calculated relate

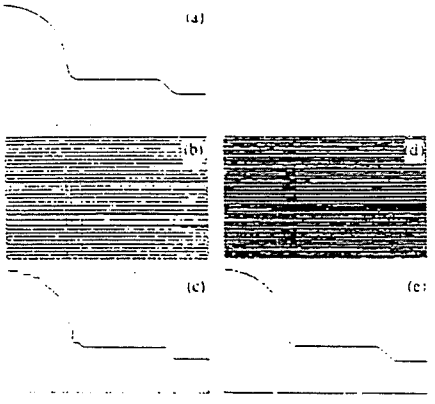

Fig. 3
Mesh a cavity by URMEL.
(a) target cavity to be meshed; (b) automatic mesh, D/d = 1:1, mesh number is 2,000; (c) the input cavity shape produced by (b); (d) D/d = 3:1, 25,000 mesh points; (e) the input cavity shape produced by (d).

to the number of mesh points. Figure 3 shows the relation between the contour of cavity inputted into URMEL and the number of mesh points. When using 2,000 mesh points [Fig. 3(b)], the contour [Fig. 3(c)] of the cavity inputted into URMEL is far away from the actual cavity contour [Fig. 3(a)]. When using 25,000 mesh points [Fig. 3(d)], the inputted cavity contour [Fig. 3(e)] closes the actual cavity contour. In Fig. 3(e), the variable mesh density technique has been used. Obviously, the latter is credible.

It is difficult to get exact E_p/E_{acc}. However, it is unnecessary to pursue absolute accuracy. In the process of searching for the optimal cavity shape, it is important to compare various cavity shapes. With the same calculation condition and credible calculation results, one can compare the cavity shapes from individual laboratories throughout the world. DESY usually calculates a multicell cavity using automatic mesh 1:1 and variable mesh density 3:1 for a single-cell cavity. We use automatic mesh 1:1 for multicell cavity and two kinds of variable mesh density (3:1 and 5:1) for a single-cell cavity.

4. CELL DESIGN AND ACCELERATING MODE CALCULATIONS

The designed single-cell cavity BSC1 is based on the LEP 4-cell cavities, the ARES 4-cell cavities, and the Cornell B-Factory (CBF) cavities [15], but as always, the ellipse at iris substitutes the circular arc, the so-called "CSE" type. LEP cavity operates at 352 MHz, ARES and CBF operate at 500 MHz. The different frequencies corresponding to different size are all scaled to 1.3 GHz, so that one can compare their shapes and physical parameters (see Table 1). Using URMEL, with 25,000 mesh points to calculate the whole single-cell cavity consisting of the welding cell and beam tube, and the obtained data are listed in Table 1. According to the DESY criterion (25,000 mesh points, D/d = 3:1), the E_p/E_{acc} of BSC1 cavity is reduced to 2.0 already. However, all practical accelerating cavities are multicell cavities, except the cavities used in the factory-type machines, the E_p/E_{acc} of the π mode in the middle cells is about ten percent higher than that in the end cells. To demand E_p/E_{acc} = 2.0 in the middle cells, it is necessary to reduce E_p/E_{acc} in the end cells to 1.8. So the 9-cell TESLA cavity was studied [12] to obtain the end cell, and BSC2 and BSC3 are formed by combining two half-end cells. Their geometrical and physical parameters are listed in Table 2 together with BSC1 for comparison. One may see from the table that BSC2 and BSC3 are satisfactory and desirable.

Table 1
Comparison of structure and accelerating mode parameters of cavities.

		CBF	LEP	ARES	BSC1
OR(mm)		105.60	102.16	102.30	102.4
R_2(mm)		31.64	45.27	45.20	45.27
TD		75°	79.48°	79.36°	79.36°
R_1(mm) or A_2(mm) B_2(mm)		7.673	7.697	7.710	 50.80 10.25
IR(mm)		46.00	38.86	38.53	38.78
L(mm)		46.00	55.79	55.88	54.81
E_p/E_{acc} (NP_{max} = 25000)	D/d = 1:1 D/d = 3:1 D/d = 5:1	2.06 – –	1.97 2.167 –	1.97 2.14 2.16	1.80 1.97 2.08
H_p/E_{acc} ((A/m) / (MV/m))		3334.3	3222.9	3207.0	3151.3
R/Q (Ω)		89.0	108.3	109.5	107.5
G		230	264	261	267

Note: — : uncalculated; H_p: maximum of the surface magnetic field; NP_{max}: the number of mesh points; R/Q: shunt impedance over Q for the accelerating mode.

Table 2
Comparison of parameters for three newly designed cavities.

		BSC1	BSC2	BSC3
OR(mm)		102.4	103.3	103.6
$A_1 = B_1 = R_2$(mm)		46.27	39.01	35.54
TD		79.36°	79.0°	79.0°
A_2(mm)		50.80	32.0	32.0
B_2(mm)		10.25	16.0	16.0
IR(mm)		38.780	39.0	39.0
L(mm)		54.81	55.6	52.8
f(MHz) (NP_{max} = 25000)	D/d = 1:1 D/d = 3:1 D/d = 5:1	1297.786 1297.536 1287.153	1299.082 1299.265 1299.504	1297.802 – –
E_p/E_{acc} (NP_{max} = 25000)	D/d = 1:1 D/d = 3:1 D/d = 5:1	1.80 1.97 2.08	1.729 1.795 1.782	1.696 – –
H_p/E_{acc} ((A/m) / (MV/m))		3151.3	3461.6	3517.3
R/Q (Ω)		107.5	106.3	106.0
G		267.0	247.5	235.0
k_0 (V/PC)		0.219	0.216	0.215

Table 3

Some physical quantities variation trend as the beam tube radius increases.

IR	E_p/E_{acc}	H_p/E_{acc}	$R(\Omega)$	$(R/Q)_{fund}$ (Ω)	$(R/Q)_{Hom}$ (Ω)	$N_{parasitic\ modes}$
↑	↑	↓	↓	↓	↓	↓

Note: ↑ indicates increase; ↓ indicates decrease.

Table 4

Comparison of physical parameters between ARES1 with tube radius variated and ARES2 with tube radius invariated.

	L_{total} (mm)	R (mm)	E_p/E_{acc}	H_p/E_{acc} ((A/m) / (MV/m))	R/Q (Ω)	$N_{monoHom}$	G	D_{TM010}
ARES1	98	$a_1 = 38.53$ $a_2 = 22.0$	2.14	3207.0	109.5	11	261	60.0
ARES2	98	$a = 38.53$	2.26	3191.1	109.0	2	260	47.3

5. DESIGN OF THE BEAM TUBE

The design of the beam tube must take several factors into consideration. The beam tube radius IR affects directly many physical parameters as shown in Table 3.

The technique of variable beam tube radius is applied in the LEP, ARES, and BSC cavities. For suppose ARES1 is with the variated tube radius and ARES2 with the invariated tube radius, using URMEL with 25,000 automatic mesh points, the data calculated are listed in Table 4 for comparison. It is easy to see from Table 4 that the most sensitive parameters of the tube radius are the number of parasitic modes, the E_p/E_{acc}, and the decay amount of the fundamental mode in the cavity. The cutoff wavelength of the TM01 mode in a circular waveguide is

$$\lambda_c = \frac{2\pi}{u_{01}} a = 2.62a\,, \tag{1}$$

here u_{01} is the first zero of the zero-order Bessel function, and a is the tube radius. Apparently, the bigger the a is, the longer the λ_c is; the less the parasitic modes are, the more the propagating modes are. The tube radius of the Cornell B-Factory cavity is deliberately designed to be so large that it enables all monopole higher order modes (HOMs) to become propagating modes which are absorbed by magnetic materials outside the cryostat. The smaller the tube radius is, the more parasitic modes there are. It is necessary for the HOM coupler near the cell to extract HOM power. In addition, the beam tube length also directly affects physical parameters. Supposing that BSC1 and BSC1* are identical except for different tube lengths, and calculating their fundamental modes using URMEL with 25,000 mesh points, the results are listed in Table 5. From Table 5, one can see that tube length affects the decay amount of fundamental modes severely, and E_p/E_{acc} slightly. In brief, the cutoff depth of fundamental mode in the beam tube depends on the radius and length of the beam tube. The damping amount of the evanescent wave in the tube is expressed as follows:

$$L = 54.5 \frac{l}{\lambda_c}\left[1 - \left(\frac{\lambda_c}{\lambda}\right)^2\right]^{1/2}, \tag{2}$$

Table 5
Parameters for different beam tube lengths in BSC1.

		BSC1	BSC1*
$L_{thick} + L_{transit} + L_{thin}$ (cm)		6.1 + 2 + 2.4	6.1 + 2 + 6.4
f(MHz) of TM010		1297.153	1296.800
E_p/E_{acc} (NP_{MAX} = 25000)	D/d = 1:1	1.80	1.803
	D/d = 4.6:1	2.08	2.02
H_p/E_{acc} ((A/m) / (MV/m))		3153.3	3153.3
R/Q (Ω)		108.0	107.6
D(db) of TM010 in tube		60	90

where L is the tube length, and λ is the vacuum wavelength of corresponding standing wave mode. The cutoff wavelength can be calculated according to Eq.(1). For the variable tube, one may calculate each segment, respectively, and for the transition segment, use the average radius in partial subsegment, and then add the damping amounts (db) in different segments together in order to obtain the total damping amount.

According to the operation experiences of superconducting cavities throughout the world, to enable fundamental mode TM010 to operate at $Q_0 = (1.5 - 3) \times 10^9$, the decay amount of TM010 in the beam tube should reach 55-60 db or so. This is a basic demand. If the technique of variable tube radius was not used to satisfy the same decay, the tube length would need to be prolonged, whereby the volume of the cryostat and the construction and operating costs may have to be increased.

In addition, for the individual cavities, sometimes there are some special considerations, such as enhancing the local field of certain HOMs in which damping is difficult in the beam tube in order to extract more power for the HOM coupler, or enhance the input coupling of the fundamental mode, etc.

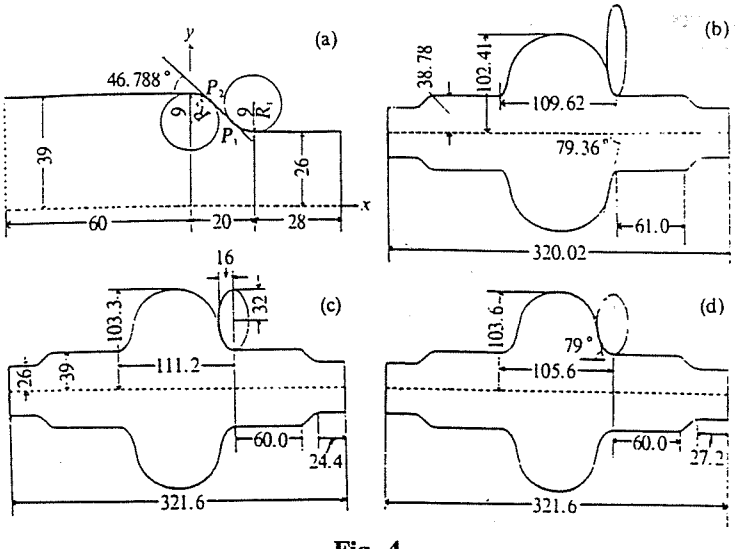

Fig. 4
The geometrical structure of BSC cavities.
(a) dimensions of beam tube; (b), (c), and (d) show the shape and dimensions of BSC1, BSC2, and BSC3, respectively.

The tube of the designed BSC cavity consists of three segments, called the thick tube, the transition segment, and the thin tube, respectively. The thick tube radius is large enough for most HOMs to enter easily into the tube so that their power can be extracted efficiently by the HOM coupler. The thin tube enables fundamental mode to attain enough decay. The transition segment runs smoothly and slowly to avoid wake and multipacting effects; here the "CSC" connection technique is applied, but two circles are with the same radius as shown in Fig. 4(a). The integrated cavity shapes, BSC1, BSC2, and BSC3 are shown in Figs. 4(b), 4(c), and 4(d), respectively.

6. CALCULATION OF HOM

6.1. Basic concept

There are infinite modes in a resonant cavity. All modes may be divided into two types: transverse magnetic field modes (TMmnl) and transverse electric field modes (TEmnl) according to their field distribution; moreover, they are classified into monopole modes, dipole modes, quadrupole modes, etc., according to the angle parameters. The monopole modes, as with the TE0-like modes, are with a zero longitudinal electrical field ($E_z = 0$); consequently, they have no energy exchange with beam bunches so they could be left out of consideration, which left only TM0-like modes. TM010 is an accelerating mode; TM011, TM020, and the above are called monopole HOMs. Dipole modes, quadrupole modes, etc., are multipole HOMs. TM110 and TM111 are the lowest modes in dipole modes. Generally speaking, all HOMs in cavities are harmful, except in crab cavities [16]. Monopole HOMs tend to introduce energy spread (within bunches and bunch to bunch). Multipole HOMs tend to cause beam transverse emittance growth so HOMs should always be damped adequately.

For an open cavity, HOM can be divided into standing wave modes and travel wave modes. Travel wave modes can propagate along beam tubes, and can be absorbed when they meet the tube wall consisting of dissipated materials outside the cryostat. Hence one should make use of low RRR (50-100) Niobium to build the beam tube. For the multicell cavities, the travel wave mode could form trapped modes under certain conditions. This is a difficult and potentially destructive problem. In general, there is no such problem in single-cell cavities. But the HOM power under the cutoff frequency needs to be extracted out of the cell with an HOM coupler.

R/Q is a physical quantity measuring longitudinal HOM behavior, and $(R/Q)''$ is another physical quantity measuring transverse HOM behavior. Its definition is

$$\left(\frac{R}{Q}\right)'' = \frac{R/Q}{(K \cdot R_0)^2}, \tag{3}$$

where the wave number $K = \dfrac{\omega}{\beta_c}$, ω is mode circular frequency, β_c is electron velocity, and R_0 is the distance away from axle of cavity.

It is likely that various random perturbations may excite one, two, or more HOM oscillations. The bunches with fixed periodic action to cavities have a wide ranging frequency spectrum. It could excite a serial of HOM oscillations. R/Q is a measure of how much energy the beam bunches deposit in the corresponding monopole HOM; similarly, $(R/Q)''$ measures the same for the multipole HOM. The higher the R/Q or $(R/Q)''$ is, the more dangerous the mode is. Deserving precautionary attention, these HOMs must be damped adequately. The damping in these cases would be that the energy is either extracted or dissipated. However, it is impossible to extract or dissipate all the energy, but only a portion. The external quality factor Q_{ext} is a physical quantity measuring damping depth. Its definition is

$$Q_{ext} = \frac{\omega U}{\Delta P_{diss}}, \tag{4}$$

where U is stored energy within the mode, and ΔP_{diss} is the power extracted by HOM coupler.

6.2. HOM load model

Many coaxial HOM couplers have been developed in Europe. Cornell University has developed a waveguidelike HOM coupler. One can calculate Q_{ext} of the coaxial HOM coupler using the URMEL code under the proper mathematical model and compare it with measured Q_{ext}. Rectangular waveguidelike HOM couples need to be calculated using the MAFIA code [17]. Here Q_{ext} of HOM is calculated using the "resistive band model" developed by Walter Hartung. URMEL, URMEL-T, and SUPERFISH codes do not allow the boundary condition of dissipation. In the resistive band model, a piece of aluminum tube near to the cell substitutes for the copper tubes as shown in Figs. 5(a) and 5(b). Though conductance of aluminum is slightly smaller than that of copper, it is still a good conductor that satisfies the conditions demanded by URMEL-T, and the computed frequency and field data shift only slightly. Here, the aluminum tube length is one inch. Its start is 3.18 millimeters away from the end of the cell. The dissipated power in the aluminum band by an individual mode is larger than that in the original copper band. The difference is

$$\Delta P_{\text{diss}} = \frac{1}{2}\left[R_s\,(\text{Al}) - R_s\,(\text{Cu})\right] \int_{\text{band}} H_\varphi^2 \, dA\,, \tag{5}$$

putting Eq.(5) into Eq.(4), the calculation formula for Q_{ext} is obtained as

$$6Q_{\text{ext}} = \frac{\omega U}{\frac{1}{2}\left[R_s\,(\text{Al}) - R_s\,(\text{Cu})\right] \int_{\text{band}} H_\varphi^2 \, dA}\,, \tag{6}$$

where H_φ is the surface magnetic field; R_s(Al) and R_s(Cu) are the surface resistance of aluminum and copper, respectively. Their definition is

$$R_s = \frac{1}{\sigma\delta}\,, \tag{7}$$

where σ is the metal conductivity, and δ is the penetrating skin depth.

Taking BSC3 as an example, the lowest 30 monopole, 30 dipole, and 30 quadrupole modes are calculated based on the aluminum band using URMEL-T with 7,000 mesh points. Their frequency distributions are shown in Fig. 5(c), R/Q, Q_{ext} and their product $R = (R/Q) \cdot Q_{ext}$, for the lowest 30 monopole modes are shown in Figs. 5(d), 5(e), and 5(f), respectively; $(R/Q)''$, Q_{ext}'' and their product $R'' = (R/Q)'' \cdot Q_{ext}''$ for the lowest 30 dipole modes are shown in Figs. 5(g), 5(h), and 5(i), respectively; $(R/Q)'$, Q_{ext}' and their product $R' = (R/Q)' \cdot Q_{ext}'$, for the lowest 30 quadrupole modes are shown in Figs. 5(j), 5(k), and 5(l), respectively.

6.3. Further discussion on the BSC3 cavity

Figure 5(c) shows the distribution of ninety HOM frequencies in the BSC3 cavity, where f_{c_0}, f_{c_1}, and f_{c_2} are the cutoff frequencies of monopole, dipole, and quadrupole modes, respectively. Seven monopole HOMs under f_{c_0}, eight dipole HOMs under f_{c_1}, and eighteen quadrupole HOMs under f_{c_2}, are all the parasitic standing wave modes. Their extracted power mainly relies on the HOM coupler. Figure 5(d) shows TM011 and TM021 with the highest R/Q which means that both of them are the most dangerous monopole modes. However, Fig. 5(e) shows Q_{ext} of the TM021 mode is very low, and the product of $(R/Q) \cdot Q_{ext} = R$ is also very low [as shown in Fig. 5(f)] (the third mode for TM021), so TM021 is not dangerous. According to R shown in Fig. 5(f), the most dangerous monopole HOMs are TM011 and TM022. The most dangerous dipole modes are TM110 and TE111 for the same reason as shown in Figs. 5(g), 5(h), and 5(i). The most dangerous quadrupole mode is TM220 (2798.05 MHz) as shown in Figs. 5(j), 5(k), and 5(l).

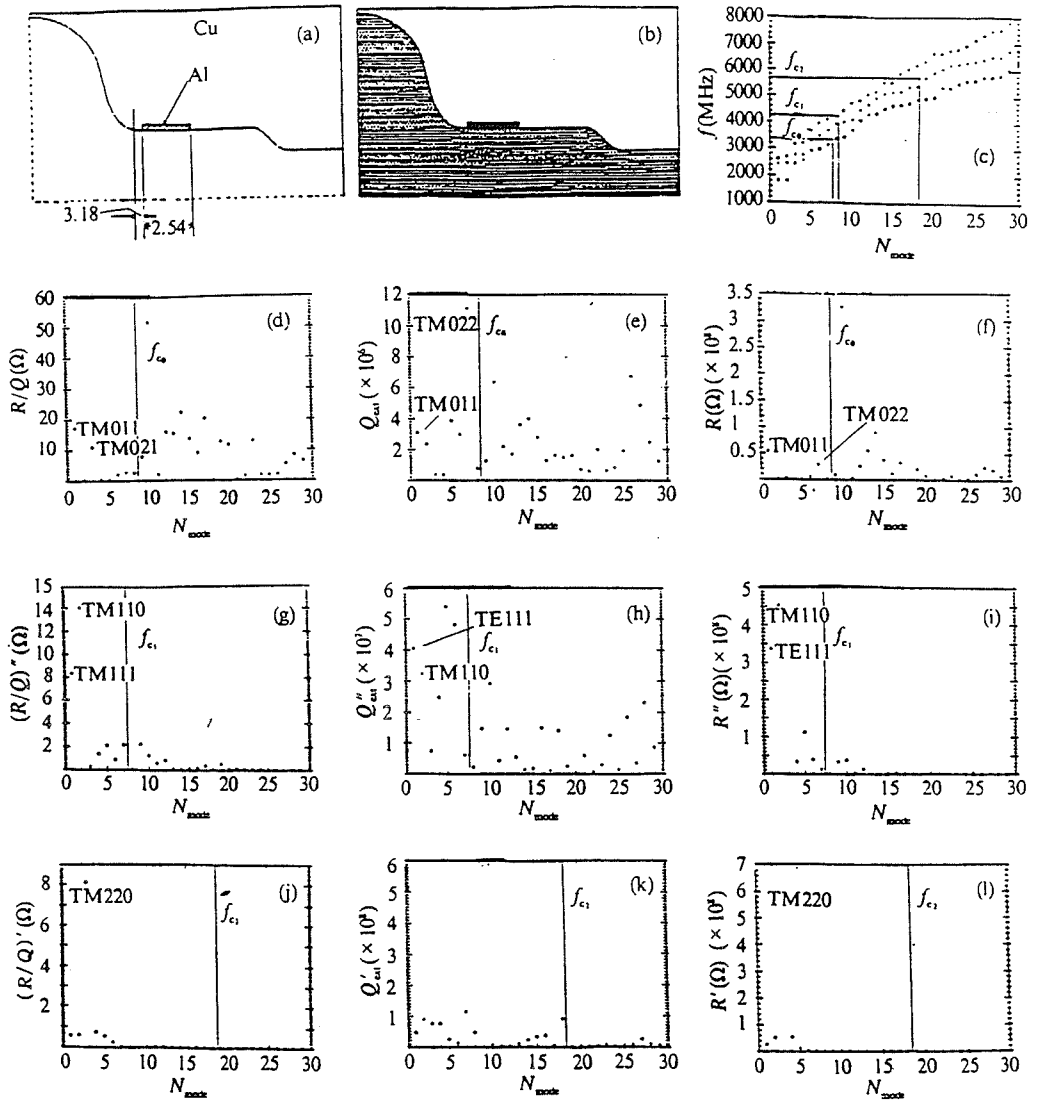

Fig. 5

HOM property of BSC3 cavity calculated based on the aluminum band model using URMEL-T with 7,000 mesh points.

(a) resistive band model; (b) mesh; (c) the frequency distribution of the lowest 30 monopole, 30 dipole, and 30 quadrupole modes. □ monopole, ○ dipole, and ◆ quadrupole. f_{c_0}, f_{c_1}, and f_{c_2} stand for the cutoff frequency of monopole, dipole, and quadrupole modes, respectively. N_{mode} denotes the sequence number of the modes; (d), (e), and (f) show R/Q, Q_{ext}, and R of the lowest 30 monopole modes, respectively; (g), (h), and (i) show $(R/Q)''$, Q_{ext}'', and R'' of the lowest 30 dipole modes, respectively; (j), (k), and (l) show $(R/Q)'$, Q_{ext}', and R' of the lowest 30 quadrupole modes, respectively.

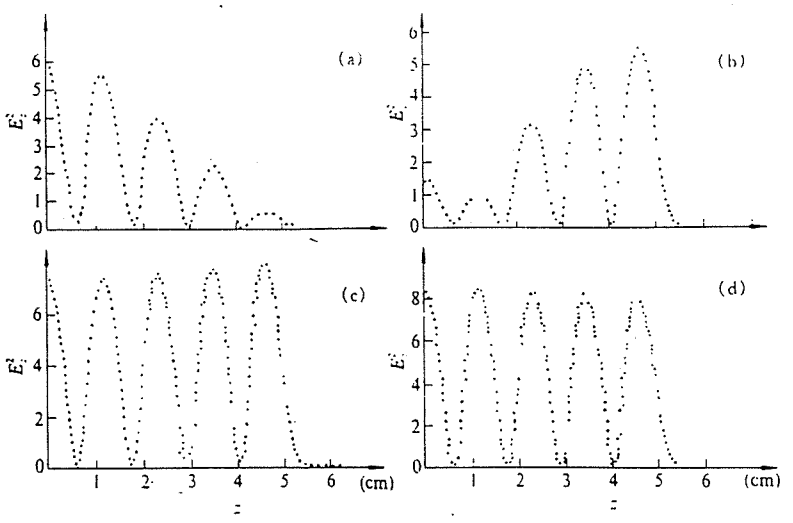

Fig. 6

The computed tuning curves (URMEL, 25,000 mesh points) of a 9-cell BT cavity, E_z^2 at axle of the cavity versus z.

(a) The mistune case when the end cell and the middle cell have the same size; (b) the tuning peak in each cell should contour, provided that *OR* of the end cell is 0.3 mm smaller than that of middle cell while keeping their L the same; (c) the perfect tuning, if *OR* is identical, half-end cell length L 52.7 mm; (d) the perfect tuning, with *OR* identical, L = 52.8 mm. E_z^2 with arbitrary unit.

A conclusion can be drawn from above discussion: for BSC3 cavity, TM011, TM022, TM110, TE111, and TM220 are all the most dangerous HOMs. Special attention should be paid to them when designing the HOM coupler.

7. CONCLUSIONS

In general, a single-cell cavity is not directly used in accelerators, except in B-Factories, for the consideration of saving expensive couplers. The attempt to design and build a single-cell cavity requires experimental investigation on cavity shape, Niobium material, couplers, and surface processing, as well as some physical effects such as FE, multipacting, etc. The so-called practical single-cell cavity is composed of two half-end cells of a practical multicell accelerating cavity. It is a contract shape of corresponding to the multicell cavity. One can use it for cavity shape study. The single-cell cavities BSC2 and BSC3 reported here are the very contracts of the 9-cell accelerating cavity newly designed by us. They can be used for both couplers for test and shape investigation. If the BT cavity ripped, one can manufacture an accelerating cavity with any number of cells between 2 and 9 with this shape.

In a multicell cavity, the geometric dimensions of half-end cells are different from that of middle cells in order to compensate the beam tube effect. If they are with the same size, their tuning curves are shown in Fig. 6(a) which is obviously a mistune state, corresponding to the nonhomogeneous

accelerating gradient in each cell. The standard way is to determine the middle cell first, then choose the half-end cell, making use of the tuning curves. In the BT cavity, the middle cell radius OR = 103.6 mm. BSC2 is obtained through tuning the BT cavity by shrinking OR of the half-end cell to 103.3 mm. URMEL does not allow boundary sharp transition. When calculating with URMEL, we input an average value of 103.6 mm and 103.3 mm, the obtained tuning curves are shown in Fig. 6(b), which may not be accurate enough. The BT cavity could be tuned carefully with the SUPERFISH code to obtain the true tuning curves and determine the exact OR.

The BSC3 cavity is obtained through tuning the BT cavity by changing half-end cell length. Figures 6(c) and 6(d) show the tuning curves for L = 52.8 mm and L = 52.7 mm, respectively, corresponding to a homogeneous distribution of the longitudinal electric field $|E_z|$ in each cell which means that the same energy is stored in each cell. This is the perfect tuning state of the multicell cavity.

In BSC2, the difference of OR between the middle cell and the half-end cell is 0.3 mm. There is no trouble when building and welding the cavity using a 2.5-3-mm-thick Niobium sheet. In the BSC3 cavity, as the half-end cell and the middle cell have the same OR, both welding and tuning are convenient; also the tuning of the BT cavity could be done easily in a computer with URMEL.

The E_p/E_{acc} in the π mode of the middle cell of the BT cavity is equal to 2.024 when BSC2 or BSC3 is used as the half-end cell of the 9-cell cavity. The cell-to-cell coupling coefficiency k is equal to 1.95%. The smaller the cell number, the larger the coupling k. If making a cavity with fewer cells than 9, the k will be larger than 2%.

ACKNOWLEDGMENTS

Dr. H. Padamsee and W. Hatrung provided some codes; Prof. C. Pagani gave the ARES cavity shape as a reference; with Dr. D. Proch we have many helpful discussions; Song Jinhu wrote an interface program between URMEL and GKS; and Prof. Chen Jiaerh and Prof. Zhao Kui contributed some support to this study. I take this opportunity to express my sincere gratitude to all of them for all their help.

REFERENCES

[1] V. Lagomarsino *et al.*, *IEEE Trans. Mag.*, **15** (1979): p. 25.
[2] P. Kneisel, *et al.*, *NIM*, **188** (1981): p. 669.
[3] C. Lyneis, *et al.*, *Appl. Phys. Lett.*, **31** (1977): p. 541.
[4] H. Padamesee and A. Joshi, *J. Appl. Phys.*, **50** (1979): p. 1112.
[5] D.L. Rubin, *Linear Collider Applications of Superconducting RF, Proc. of the 1st TESLA Workshop, 23-26 July 1990, Cornell Univ., USA.*
[6] H. Padamsee, *et al.*, *Superconducting RF Activities at Cornell University, Proc. of the 3rd Workshop on RF Superconductivity, Argonne, Illinois (1988), USA.*
[7] R.M. Sundelin, *IEEE Trans. on Nuclear Science*, **NS-32** (1985): p. 3570.
[8] Q.S. Shu, *et al.*, *Reducing Field Emission in Superconducting RF Cavities for the Next Generation of Particle Accelerators*, CLNS 90/1020, Cornell Univ., (1990), USA.
[9] J. Graber, *et al.*, "A World Record Accelerating Gradient in a Niobium Superconducting Accelerator Cavity," *Proc. of the 1993 IEEE PAC, Washington, DC*, p. 892 (1993).
[10] T. Weiland, *NIM*, **216** (1983): p. 329.
[11] U. Laustroer, U. van Rienen, and T. Weiland, *DESY* M-87-03 (1987), Germany.
[12] Donglin Zu and Jiaerh Chen, *Proc. of the 1993 IEEE PAC, Washington, DC*, p. 1095 (1993).
[13] K. Halbach and R.F. Holsinger, *Part. Accel.*, **7** (1976): p. 213.

[14] Donglin Zu, *Summary of URMEL(T) Calculations on Crab Cavity*, CLNS 91-1090, Cornell Univ., USA.

[15] H. Padamsee, *et al.*, "Superconducting RF Accelerating and Crab Cavities for the Cornell B-Factory, CESR-B, CLNS90-1039," an internal report at the Laboratory of Nuclear Studies, Cornell Univ., USA.

[16] H. Padamsee, *et al.*, *Crab Cavity Development for the Cornell B-Factory, CESR-B, PAC, San Francisco, 1991.*

[17] T. Weiland, *IEEE Trans. Nucl. Sci.*, NS-**32** (1985): p. 2738.